Electronic Supplementary Material (ESI) for Nanoscale Horizons.

Smart textiles of MOF/g-C_3N_4 nanospheres for chemical warfare agent rapid detection/detoxification

Dimitrios A. Giannakoudakis,[a,b] Yuping Hu,[a,c] Marc Florent,[a] and Teresa J. Bandosz[a,b*]

a. Department of Chemistry, The City College of New York, New York, NY 10031 USA Tel.:(212)650-6017; Fax: (212)650-6107, E-mail: tbandosz@ccny.cuny.edu

b. Ph.D. Program in Chemistry, The Graduate Center of the City University of New York, New York, 10016, USA

c. on leave from College of Chemistry and Chemical Engineering Guangxi University for Nationalities, Nanning, 530006, China and Guangxi Key Laboratory of Chemistry and Engineering of Forest Products, Nanning, 530006, China

EXPERIMANTAL SESSION

MOF and composites synthesis details. A solution of copper nitrate hemipentahydrate (2.5 g) and 1,3,5 benzenetricarboxylic acid (1.25 g) in N,N-dimethylformamide (DMF, 22 mL) was stirred and sonicated for 5 min. Ethanol (22 mL) was then added and the mixture, was stirred and sonicated for 5 min. After a further addition of 22 mL of deionized water and stirring for 5 min, 0.25 g of gCN or gCNox were added to the mixture, which was sonicated for 30 min. All crystals were dissolved at this point. The mixture was then transferred to a round bottom flask and heated at 90 ^{o}C in an oil bath for 21 h under shaking (strongly for the first 4 h, then the shaking was reduced and stopped after 20 h). After cooling, the crystals were collected on a filter, and finally washed and immersed in dichloromethane. Dichloromethane was changed twice during three days. Drying of the crystals was performed by heating them at 120 ^{o}C for 28 h inside a closed

filtering flask connected to vacuum. The Cu-BTC sample is referred to as MOF, while the composites with gCN or gCNox are referred to as MOFgCN and MOFgCNox, respectively.

Procedure of textiles modification: 60 mg of the active phase was dispersed in ethanol via sonication for 15 minutes. A cotton textile (~300 mg) was introduced to this suspension for 5 minutes and then was placed on a heated plate (75 ^{o}C). The heated textile was covered by active phase suspension in ethanol in successive steps (after solvent evaporation in every step) until all material was deposited on the surface. Afterward, the textiles were dried in an oven at 100 ^{o}C overnight (16 hours). Finally, the textiles were mechanically fold/unfold and exposed to a pressurized air stream for 3 minutes, in order to remove the weakly attached MOF/composites. The obtained color was dark blue for all three samples. Exposure of the textiles to ambient conditions, changed color to light blue/turquoise (Figure s1). When the textiles were placed again to the oven, the color returned to the dark blue, as a result of the removal of the weakly adsorbed water. This color change occurred even when the textiles where left at ambient conditions for more than 15 days, supporting indirectly the stability of our samples. It is worth to mention that the color of the MOF based modified textile was darker than those with the composites deposited on the cotton fibers. The received textiles with deposited MOF, MOFgCN, and MOFgCNox are referred to as T-M, T-MG, and T-MGox, respectively.

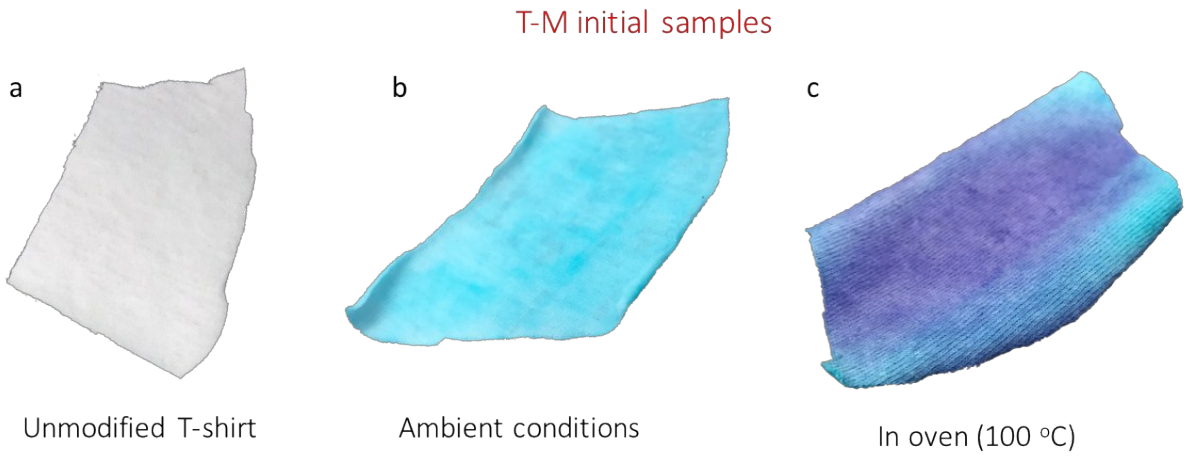

Figure s1. Photographs of the textiles. a, initial cotton textile. **b,** T-M under ambient conditions. **c,** T-M textile after removed from the oven.

Vials-in-Vial reactive adsorption system. The reactive adsorption of DMCP was studied in batch experiments using a homemade close vial system (Figure s2), at ambient light or in the dark. Two 1 mL reaction vessels were placed in a 20 mL glass vial. In the first vessel, 20 mg of sample was inserted before the addition of DMCP and the vial was tightly capped with a septum. Through the septum, 40 μL of DMCP was injected into the second reaction vessel. The vessels were kept at ambient temperature from 24 to 192 hours, depending on the target exposure time. The vapor phases from the headspace of the glass vials were sampled with a syringe at specified time periods and injected into GC-MS. Then, the containers were opened to equilibrate the adsorbents for 1 h at dry conditions and ambient temperature. The reaction vessels containing the samples were weighed and the change in weight was recorded.

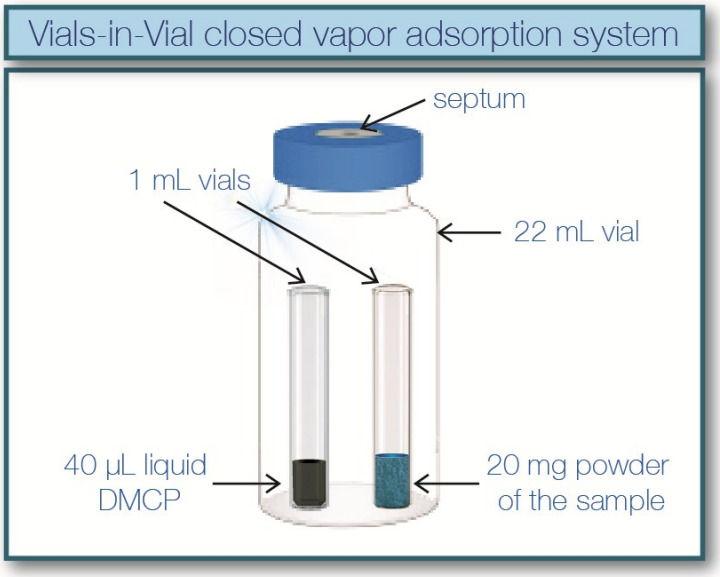

Figure s2. Vials-in-Vial closed vapor adsorption system.

Monitoring the NO_x in the headspace. The analysis of NO_2 and NO concentration in the headspace was performed by sampling 3 mL of the headspace and injecting it into a RAE Multirae Plus monitoring system with an electrochemical sensor

FT-IR Spectroscopy. The Fourier transform infrared (FTIR) spectra were obtained using a Nicolet 380 spectrometer using the attenuated total reflectance (ATR) accessory. The spectrum was collected 64 times between 4000 and 600 cm^{-1} with background correction.

Powder X-Ray Diffraction (XRD). XRD patterns were obtained on a Phillips X'Pert X-ray diffractometer with powder diffraction procedure, using a $Cu_{K\alpha}$ radiation (operated at 40 kV and 40 mA). The diffraction patterns were collected from a 10 to 70° 2θ.

Simultaneous Thermal Analysis – Mass Spectroscopy (TA-MS). Thermogravimetric (TG) curves were measured on a SDT-Q600 (TA Instrument, New Castle, DE, USA) in helium (at 100

mL / min) with heating rate 10 ^{o}C/minute from ambient temperature to 1000 ºC. For the analysis both TG and derivative thermogravimetric curves (DTG) were used. Simultaneously, gases and vapors released with an increasing temperature were analyzed with a ThermoStar Gas Mass Spectrometer (GSD; Pfeiffer Vacuum). The released off-gases were scanned with a secondary electron multiplier detector. The m/z thermal profiles were collected. All the initial samples/materials were also analyzed in air to determine the copper content.

Determination of porosity. Nitrogen isotherms were measured using an ASAP 2020 (Micromeritics) at -196 ^{o}C. Samples were outgassed at 120 ^{o}C to 10^{-4} Torr before the measurements. The surface area, S_{BET} (Brunauer–Emmet–Teller method was used), the micropore volume, V_{mic} (calculated using the Dubinin–Radushkevich approach), the mesopore volume, V_{mes}, and the total pore volume, V_t (calculated from the last point of the isotherms based on the volume of nitrogen adsorbed) were calculated from the isotherms. The volume of mesopores, V_{mes}, represents the difference between the total pore volume and the micropore volume. Non-Local Density Functional Theory (NLDFT) was used to calculate the pore size distributions (free download at http://www.nldft.com).[1,2]

Scanning electron microscopy (SEM). The morphology of the materials was investigated with a Zeiss Supra 55 VP (accelerating voltage of 5.00 kV). The used powder or textiles were coated with 5 nm of gold.

RESULTS

The parameters of porous structure calculated from the nitrogen adsorption isotherms using the NLDFT model are presented in Figure s3 [3]. The micropore volume represent 90 %, 88 % and 49 % of the total pore volume for MOF, MOFgCN and MOFgCNox, respectively.

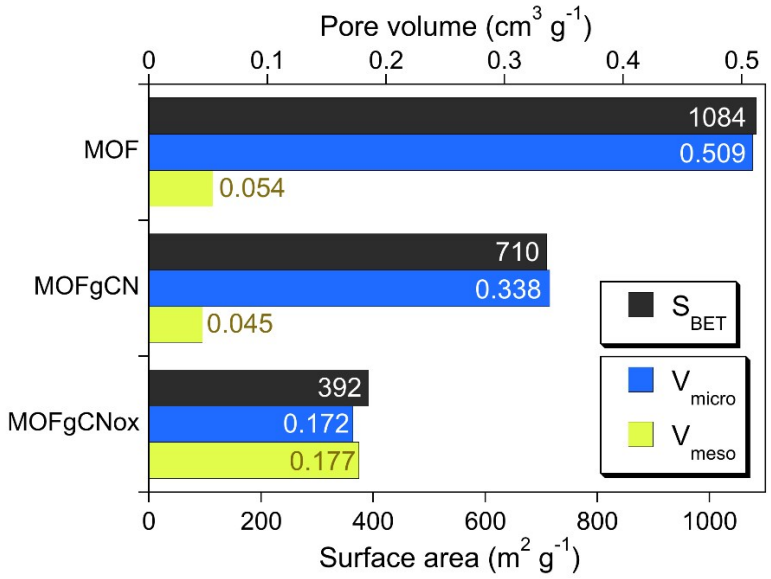

Figure s3. Porosity. The parameters of porous structure calculated from nitrogen adsorption isotherms using the NLDFT model[3].

The dispersed gCN nanosized layers and the existence of the oxidized nanospheres in the framework of MOFgCNox, as well as the incorporation of chemically active groups at the edges of these layers, play a crucial role in the photocatalytic behavior of the composite.[3] In the dark, the addition of gCN or gCNox does not cause an increase in the amount adsorbed. On the contrary, a decrease is noticed due to the decrease in the porosity.

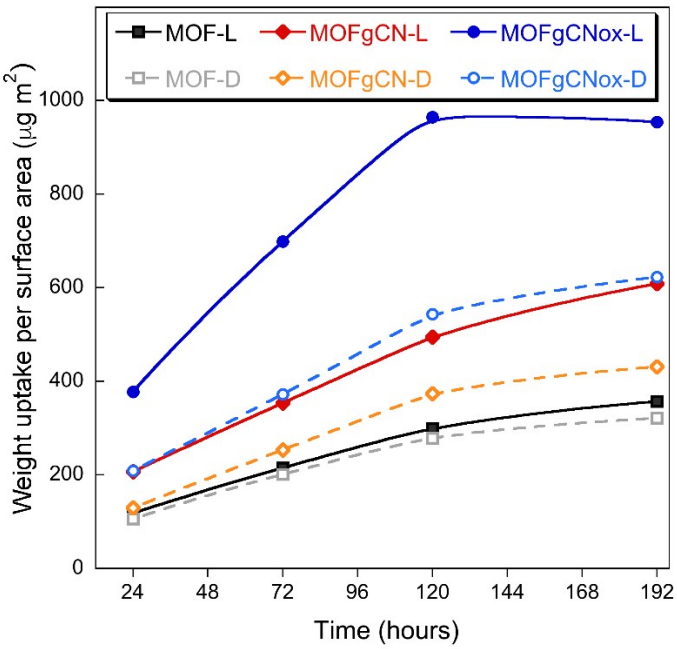

Figure s4. Weight uptakes after exposure to DMCP vapors. Evolution of the mass uptakes per surface area for up to 192 hours (-L: experiments at light, -D: in the dark).

Figure s5 shows the measured concentrations of the NO_2/NO in the headspace of the closed adsorption system at light or in the dark, at various exposure times. The limit of the detector is 100 ppm for NO_2 and 200 ppm for NO.

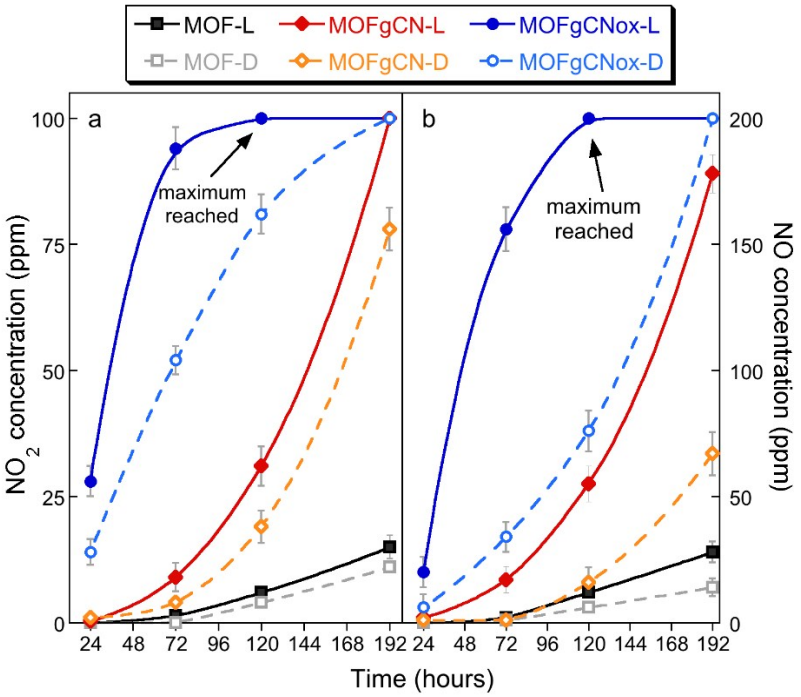

Figure s5. NO_x release during the DMCP exposure. Concentrations of NO_2 and NO in the headspace of the adsorption systems measured up to 192 hours.

The FTIR spectra of all studied samples before and after exposure to DMCP vapors are collected in Figure s6. For all initial samples, three characteristic regions of the symmetric stretching, asymmetric stretching and wagging out-of-plane bending vibration of the non-ionized carboxylic groups of the organic ligand are seen. For the composites, three additional bands appear. They are assigned to the full condensed trigonal C–N(–C)–C units, partial condensed bridging C–NH–C units, and out-of-plane bending vibrations of the heptazine or triazine ring system. It is worth mentioning that the coordination of Cu with oxygen and/or nitrogen atoms of the carbon nitride layers can be seen at the spectrum of the initial MOFgCNox, as described previously.[3]

The comparison of the FTIR spectra of the initial samples and those exposed to DMCP vapors for various times revealed numerous new bands. The spectrum of MOF exhibits several

characteristic bands related to the vibrations of the non-ionized carboxylic groups of the organic ligand in three regions: 1670-1500, 1460-1300 and 760-700 cm^{-1}. More precisely, following the previous assignment,[3] the first region represents the symmetric stretching vibrations of the carboxylic groups, having two maxima at 1644 and 1544 cm^{-1}, while the second region represents the asymmetric stretching vibrations with the maxima at 1440 and 1370 cm^{-1}.[4–6] The third region of bands at lower wavenumber, is related to the wagging out-of-plane bending vibrations of the carboxylic groups, with two sharp maxima at 759 and 726 cm^{-1}.[4–6] For MOFgCN, three additional bands originating from the graphitic carbon nitride phase appeared at 1312, 1227 and 806 cm^{-1}. They are attributed to the fully condensed trigonal C–N(–C)–C units, partial condensed bridging C–NH–C units, and out-of-plane bending vibrations of the heptazine or triazine ring system, respectively.[7,8] The spectrum of MOFgCNox showed a lower intensity of the band originating from the partially condensed units. We showed in our previous study that these units were oxidized[7]. It is worth mentioning that the band at 667 cm^{-1} can be linked to the coordination of Cu with oxygen and/or nitrogen atoms of the carbon nitride layers.[3]

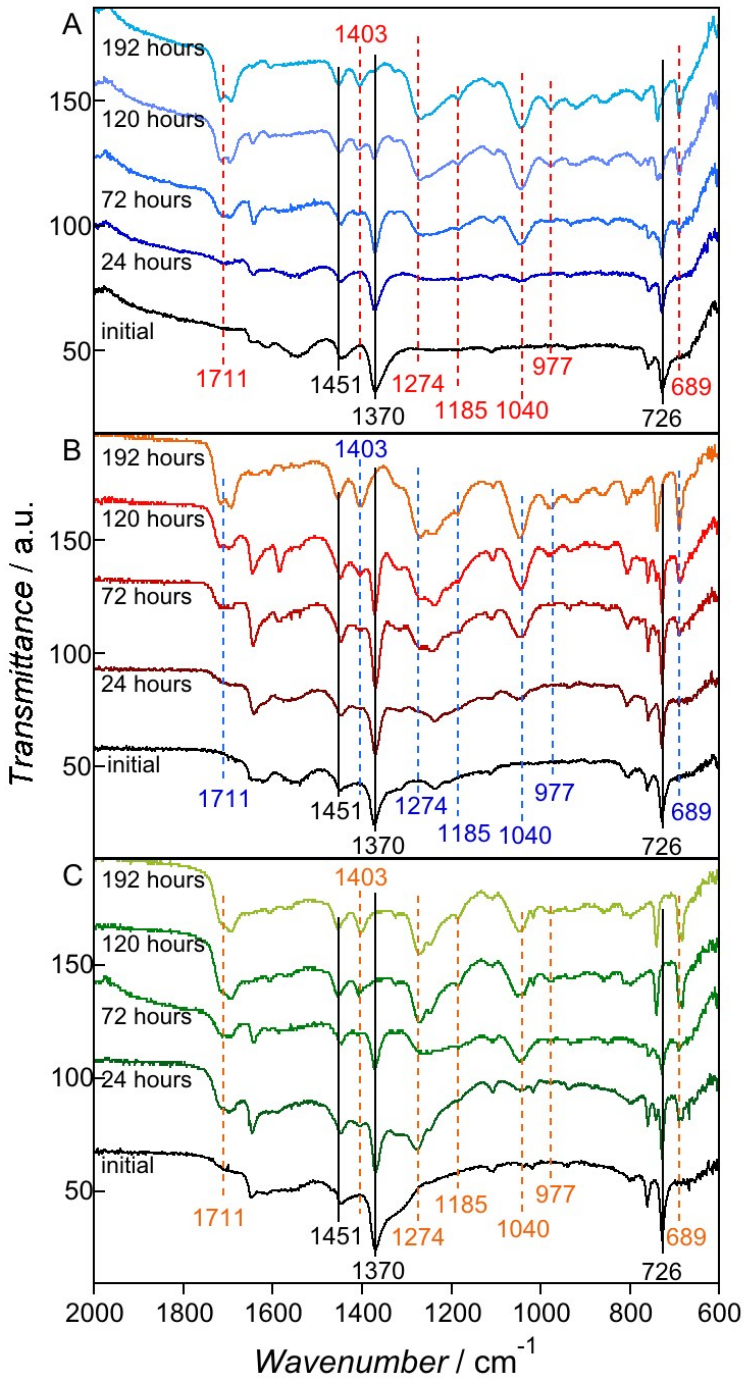

Figure s6. FTIR analysis. The spectra for MOF and its composites with gCN and gCNox, before and after exposure to DMCP for various times.

For MOF exposed to DCMP, the intensity of all the bands linked to the carboxyl groups decreased progressively, and they totally disappeared after 192 hours of exposure. On the contrary, the new bands at 1692, 1603, 1451, 1403 and 737 cm^{-1}, with gradual increase in their intensities are detected. They originate from the non-ionic form of the uncoordinated form of the framework's BTC units.[5] Moreover, the formation of the acidic form of BTC is demonstrated by the appearance of two bands at 1714 and 922 cm^{-1}. The first one could be linked to the symmetric stretching vibration of the C=O bond and the second one to the in-plane scissoring bending vibration of the O-H bond. This red shift of the bands linked to BTC, and the acidic form of the amorphous phase after the collapse of the Cu-BTC framework, was also observed by Petit et al. and linked to the interaction of Cu-BTC with H_2S.[6] The spectrum of the composite with gCNox exposed to DCMP for 120 hours does not show initial bands of the coordinated BTC, suggesting that the structure collapsed faster than that of MOF or MOFgCN. The bands related to the gCN phase became more intense with an increase in the exposure time. This further supports the collapse of the framework during the interactions with DMCP vapors.

The FTIR spectra of DMCP in liquid and gaseous phase, as well as the assignments of the bands, are shown in Fig. s7. For the exposed materials, the characteristic bands of DMCP at 1451, 1274, 1185, 1097 and 1044 cm^{-1} (Figure s6) start to appear on the spectra even after the first 24 hours of exposure, and their intensity gradually increases. Details about the assignments of these bands are collected in Table s1. The bands related to the acidic form of hydrolyzed dimethyl phosphate (DMP) and the band representing the Cu-Cl bond at 689 cm^{-1} increase in their intensity with an increase in the exposure time. The low intensity bands at 1322 and 918 cm^{-1} originating from $\delta(CH_3P)$ and $\rho(CH_3P)$ vibration, respectively, suggest that methanolysis is also one of the decomposition paths. A characteristic band at 1021 cm^{-1}, which is assigned to methanol, is

observed only on the IR spectrum of the composite with the oxidized graphitic carbon nitride. It supports the higher surface reactivity of gCNox, which leads to the decomposition of methyl groups of the adsorbed molecules and their release as methanol. The FTIR analysis indicates that that the vapors of DMCP after initial adsorption on the surface gradually undergo hydrolysis and/or methanolysis, with the simultaneous collapse of the Cu-BTC framework.

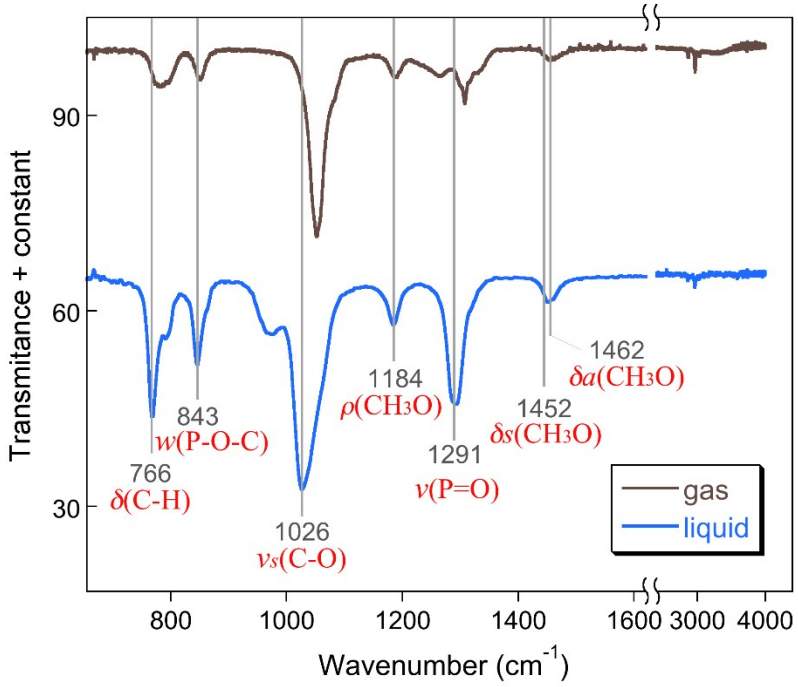

Figure s7. FTIR analysis of the pure surrogate. The spectra of the liquid and gaseous form of DMCP.

Table s1. Assignments of the IR bands of the fresh and spent sample exposed to DMCP for 192 hours.

Mode	fresh	Spent	citation
v_s(C=O)	-	1714	[4–6]
v_s(COO^-)	1644	1692	[4–6]
v_s(COO^-)	1554	1603	[4–6]
v_{as}(COO^-)	1440	1451	[4–6]
v_{as}(COO^-)	1370	1403	[4–6]
δ_s(O-H)	-	922	[4–6]
ω(COO^-)	759	774	[4–6]
ω(COO^-)	726	737	[4–6]
C–N(–C)–C	1312	1312	[7,8]
C–NH–C units	1227	1227	[7,8]
out-of-plane bending vib.	806	806	[7,8]
δ(CH_3O)	-	1451	[9–11]
v(P=O)	-	1274	[9–11]
ρ(CH_3O) and ρ(CH_3P)	-	1185	[9–11]
v_{as}(C-O)	-	1097	[9–11]
v_s(C-O)	-	1044	[9–11]
v(P-OH)	-	977	[10,12]
δ(P-OH)	-	939	[10,12]
δ(CH_3P)	-	1322	[9,11,13]
ρ(CH_3P)	-	918	[9,11,13]
v(CH_3-OH)	-	1021	[13]
v(Cu-Cl)	-	689	[10,14]

The Differential Thermal Gravimetrical (DTG) curves in helium of the initial samples and those exposed to DMCP vapors for 192 at light are collected in Figure s8. For the initial MOF, three decomposition peaks at 70, 210 and 340 °C are revealed on the DTG curve. The latter is the major one, representing the collapse of the framework.[3,15] The peak at 70 °C corresponds to the

release of physically adsorbed water, while the peak at 210 ^{o}C- to the limited impurities of unreacted $Cu(NO_3)_2$.[3,10,15] For the composites, the decomposition of the graphitic carbon nitride phase occurs above 600 ^{o}C.[7]

For MOF exposed to DCMP for 8 days at ambient light, the major/characteristic peak on the DTG curve at 340^{o}C slightly decreased in its intensity. Its presence indicates the limited decomposition of the MOF framework after exposure. Interestingly, this peak almost disappeared for MOFgCN and is not detected for MOFgCNox. This further supports the collapse of the framework during the adsorption and it is in good agreement with the XRD, SEM and FTIR results and with the observed changes in samples' color after DMCP exposure. In the case of the composites, the absence of the peak at 70 ^{o}C related to the removal of water is linked to the participation of H_2O in the photo induced surface reactions. That water likely provides the hydrogen and/or hydroxyl radicals formed as a result of electron/hole pairs generation on the photoreactive gCN phase. For all three samples, a broad peak on DTG curves starting between 100 ^{o}C and 310 ^{o}C is assigned to the decomposition of a variety of new species formed as a result of reactivity. They are removed from the surface upon heating.

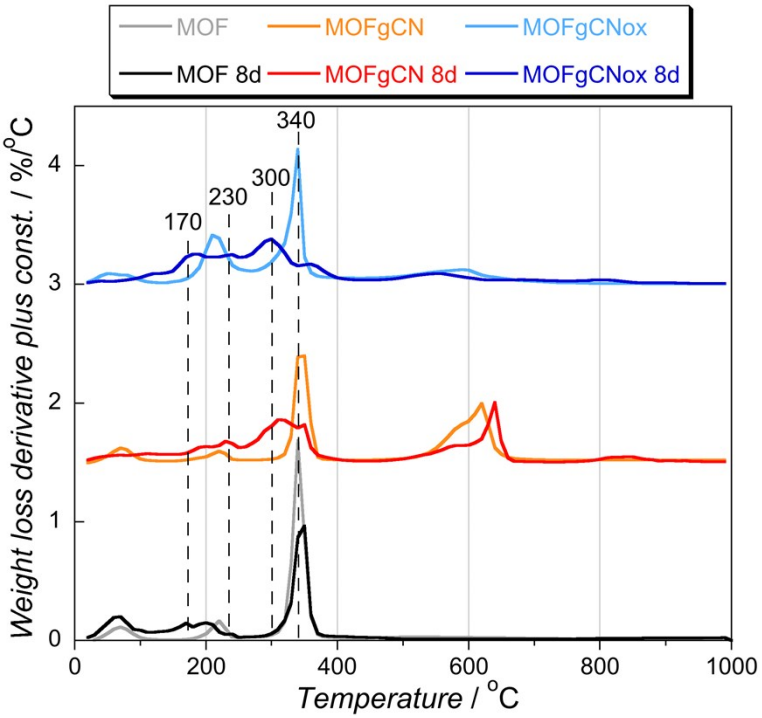

Figure. s8. Thermal analysis. Differential Thermal Gravimetrical curves in helium for the initial sample and those exposed to DMCP for 192 hours.

To identify the nature of the peaks on the DTG curves, the m/z thermal profiles of the species released during the thermal analysis were analyzed (Figure s9). The mass fragmentation spectra of all the identified compounds were obtained from the National Institute of Standard and Technology library. The m/z 47 was selected for the identification of DMCP and DMP. Considering that the boiling point of DMCP is 80 ºC, a broad peak between 80 and 310 ºC with two intense maxima on the m/z 47 thermal profile suggests that DMCP vapors are not only physically adsorbed in the pores by dispersive forces but some specific interactions such as hydrogen bonds or polar forces are also involved. Two maxima on m/z 35 (related to chloride) thermal profile at around 130 and 200 ºC support the interaction of DMCP molecules with surface centers of different energies. The broader peaks on m/z 47 thermal profile than those on

m/z 35 suggest the presence of DMP and other degradation byproducts. This is further supported by similar trends in the features of the thermal profiles of C and -CH_3 (m/z 12 and 15, respectively). The peak at 230 ^oC on the thermal profile for m/z 35 is linked to the decomposition of $Cu_2(BTC)_3Cl$ unit of the framework. Tribasic copper chloride decomposes to HCl and CuO at 220 ^oC. The thermal profile of –OH originating from water reveals a peak at 70 ^oC, only for pure MOF, as discussed above. Finally, the thermal profiles of m/z 31 support the presence of strongly adsorbed methanol. The intensity of this m/z is significantly higher for MOFgCNox than for MOFgCN. m/z 31 is not detected for MOF.

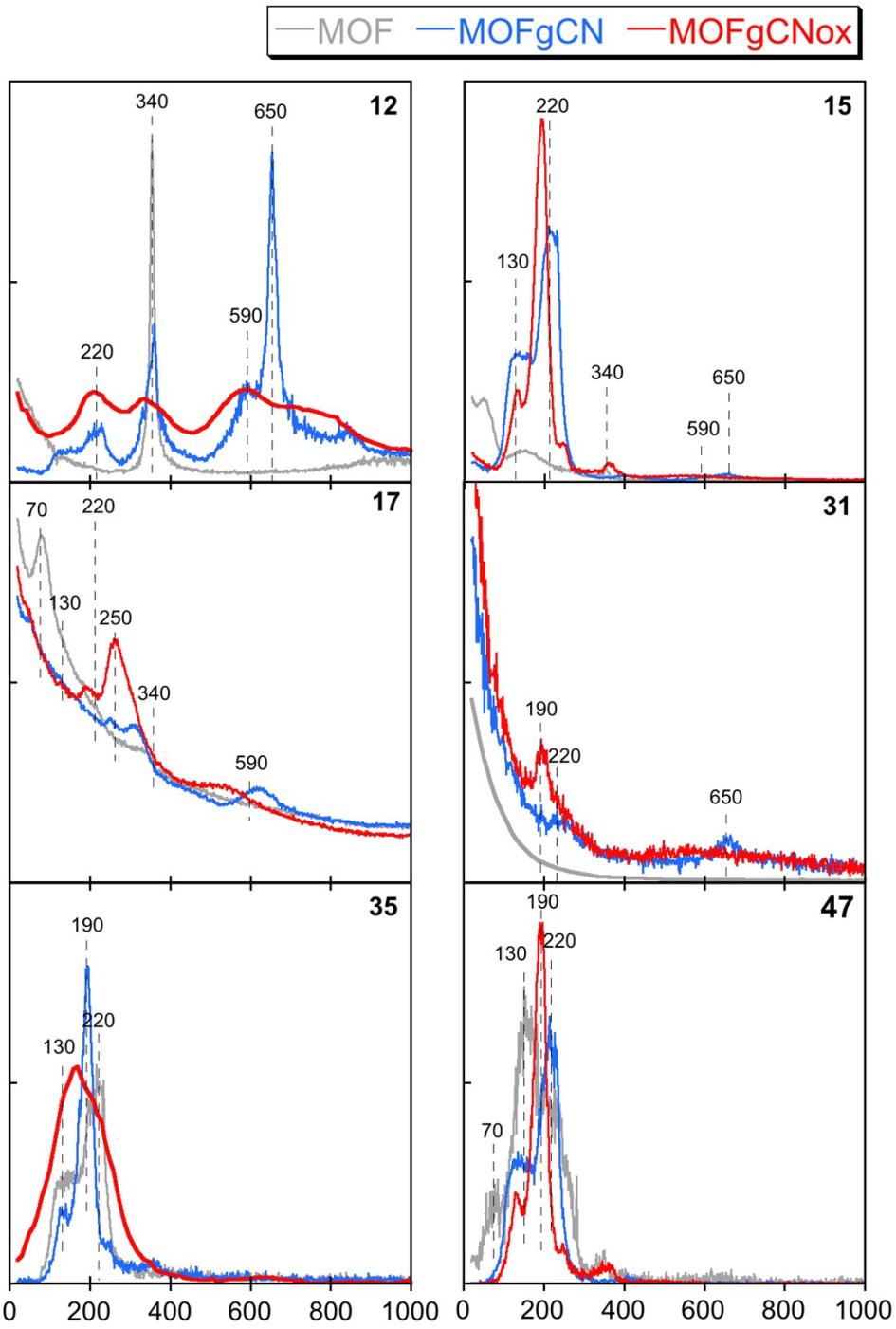

Figure s9. MS analysis of the species released from the samples during thermal analysis. m/z thermal profiles (in helium) for the fragments related to C (m/z: 12), -CH_3 (m/z:15), -OH (m/z:17), methanol (m/z:31), Cl (m/z:35), DMCP (m/z:47) for the samples exposed to DMCP for 8 days at light.

HYBRID COTTON TEXTILE (T-shirt)

The amounts of copper in the powder samples and on the textiles were determined by thermal analysis up to 1000 ^{o}C in air[3]. The amounts of the weight remaining (in wt %) are collected in Table s2. Assuming that these species represent copper oxide, CuO, the amount of copper (Cu/CuO = 0.80) on the textiles was between 0.63 and 2.04 %, while the amount of copper in the powder samples was between 19.5 and 27.6 %.

Table s2. The amounts of the remaining samples after the thermal analysis in air, and the calculated amount of copper – in wt %.

sample	remaining sample	Cu
MOF	34.52	27.6
MOFgCN	24.51	19.6
MOFgCNox	24.43	19.5
T-M	1.95	1.56
T-MG	2.55	2.04
T-MGox	0.79	0.63

The weight uptakes of the textiles expressed as mg g^{-1} are collected in Fig. s10. The textiles were exposed to 18 hours at ambient conditions prior the detoxification tests.

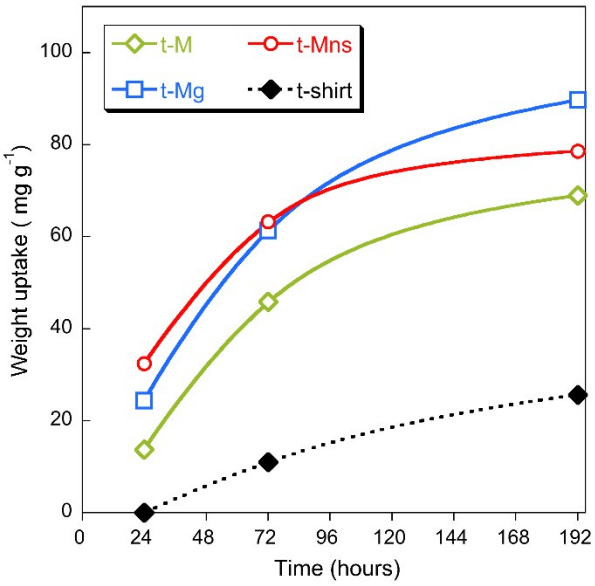

Fig. s10. Weight uptakes on the textiles. The recorded weight uptakes for all the tested textiles after exposure to DMCP vapors at various times in visible light.

The normalized weight uptakes per gram of copper (WU_{pCu}) for the modified textiles were calculated using the equation s1, where WG_S is the weight uptake of the sample, WG_T -the weight uptake of the pure T-shirt after the corresponding exposure time, and Cu% - the amount of copper from Table s2. For the powders, the same equation was used, and WG_T factor equals to zero.

eq. s1: $WU_{pCu} = (WG_S - WG_T) / (10 * Cu\%)$, unit: g g^{-1}

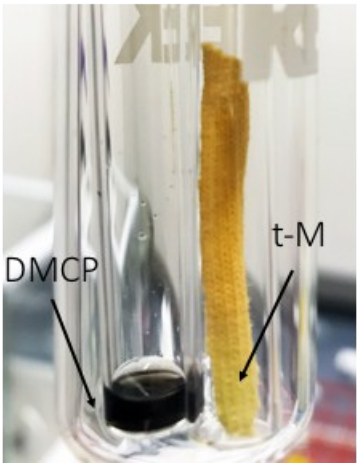

Figure s11. Decolorization of the textiles. A close caption of the T-M exposed to DMCP for 3 hours at light irradiation.

The rapid and high adsorption/catalytic DMCP detoxification, the color and surface chemistry changes, and the selectivity to DMCP of the impregnated textiles are important assets for their application as reactive adsorbents and detectors, which can simultaneously monitor the exhaustion level. It is important to point out that all formed products are nontoxic, except NO_x which was detected at low concentration and which reacts rapidly with DMCP. Moreover, MOFgCNox could be applied to different supports besides cotton for alternative applications.

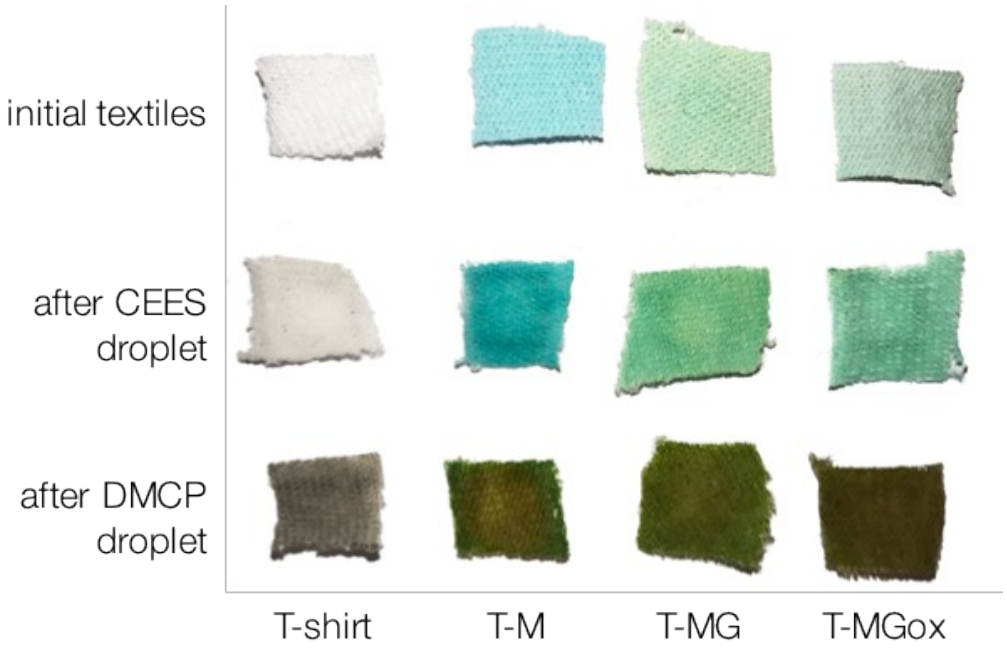

Figure s12. Direct exposure to the surrogates (droplet test). The color of all the tested textiles before and after exposure to a droplet (10 μL) of CEES and DMCP.

BIBLIOGRAPHY

1 J. Jagiello and J. P. Olivier, *Adsorption*, 2013, **19**, 777–783.

2 J. Jagiello and J. P. Olivier, *Carbon*, 2013, **55**, 70–80.

3 D. A. Giannakoudakis, N. A. Travlou, J. Secor and T. J. Bandosz, *Small*, 2017, **13**, 1601758.

4 S. Maiti, A. Pramanik, U. Manju and S. Mahanty, *ACS Appl. Mater. Interfaces*, 2015, **7**, 16357–16363.

5 A. M. Ebrahim, J. Jagiello and T. J. Bandosz, *J. Mater. Chem. A*, 2015, **3**, 8194–8204.

6 C. Petit, B. Mendoza and T. J. Bandosz, *ChemPhysChem*, 2010, **11**, 3678–3684.

7 D. A. Giannakoudakis, M. Seredych, E. Rodríguez-Castellón and T. J. Bandosz, *ChemNanoMat*, 2016, **2**, 268–272.

8 S. Pande, P. Fageria, R. Nazir, S. Gangopadhyay and H. Barshilia, *RSC Adv.*, 2015, **5**, 80397–80409.

9 A. R. Wilmsmeyer, J. Uzarski, P. J. Barrie and J. R. Morris, *Langmuir*, 2012, **28**, 10962–7.

10 J. A. Arcibar-Orozco, D. A. Giannakoudakis and T. J. Bandosz, *Adv. Mater. Interfaces*, 2015, **2**, 1–9.

11 M. B. Mitchell, V. N. Sheinker and E. A. Mintz, *J. Phys. Chem. B*, 1997, **101**, 11192–11203.

12 W. W. Rudolph, *Dalt. Trans.*, 2010, **39**, 9642–9653.

13 J. M. Bowen, C. R. Powers, a E. Ratcliffe, M. G. Rockley and a W. Hounslow, *Environ. Sci. Technol.*, 1988, **22**, 1178–81.

14 W. Martens, R. L. Frost and P. a. Williams, *Neues Jahrb. für Mineral. - Abhandlungen*, 2003, **178**, 197–215.

15 C. Petit, B. Mendoza and T. J. Bandosz, *Langmuir*, 2010, **26**, 15302–15309.